JOURNAL OF COMPUTATIONAL PHYSICS 28, 103–114 (1978)

Note

A Fourier Analysis of Some Difference Schemes for the Laplace Equation in a System of Rotational Symmetry

Fourier techniques are used to investigate some difference schemes for the Laplace equation $\Delta u(r, z) = 0$ in cylindrical coordinates. It is shown that any errors in the boundary data will give rise to a "boundary layer" around the symmetry axis, when boundary values are given on this axis, instead of using the symmetry condition. The star 5-, star 9-, and compact 9-point formulas with symmetry at the axis are also compared. The first one is the least accurate, while the compact scheme is better by at least a factor of 100 than the star 9-point scheme for the stepsize $h = 1/20$.

1. Introduction

We will use Fourier techniques to investigate some difference schemes for the Laplace equation

$$\frac{\partial^2 u(r, z)}{\partial r^2} + \frac{1}{r} \cdot \frac{\partial u(r, z)}{\partial r} + \frac{\partial^2 u(r, z)}{\partial z^2} = 0 \tag{1}$$

in cylindrical coordinates, where the z-axis is the axis of symmetry. These schemes have been much used, e.g., in numerical electron optics.

First we consider the usual star 5-point formula when we give boundary values on the z-axis, instead of using the symmetry condition

$$\partial u(0, z)/\partial r = 0. \tag{2}$$

The corresponding mathematical problem is then overdetermined by the new boundary values. It is shown that any errors in the boundary data will give rise to a "boundary layer" around the z-axis. The method with the extra boundary conditions was used by Groth *et al.* [1, 2] and Besev *et al.* [3] in calculations on magnetic lens spectrometers.

In Section 3 we consider the broad star 9-point formula and the compact 9-point formula with symmetry at the z-axis. A comparison with the star 5-point formula shows that the broad scheme is significantly better. The compact scheme is in its turn at least a factor of 100 better than the broad star 9-point formula. The latter formula has been extensively used by Natali *et al.* [4, 5] in calculations on electric two-tube lenses.

A classical text which discusses finite difference methods for elliptic equations is Forsythe and Wasow [6].

0021-9991/78/0281-0103$02.00/0

2. The Effect of Using the Symmetry Axis as a Boundary

We will here study the difference solution to the star 5-point formula for the Laplace equation (1), with boundary values $u(0, z)$ given also on the z-axis. Note that a curve in the (r, z)-plane which starts and ends on the z-axis, but does not include this, is a closed boundary of the region, because of the rotational symmetry around the z-axis. The mathematical problem is therefore overdetermined by the boundary values $u(0, z)$ and does not have any solution, which we will demonstrate below.

Let $v(k, l)$ be an approximation to $u(r, z)$, where $r = k \cdot h$, $z = l \cdot h$. The star 5-point formula for Eq. (1) is for $k \geqslant 1$

$$\begin{aligned}&(v(k+1, l) - 2 \cdot v(k, l) + v(k-1, l))/h^2 \\ &\quad + (v(k+1, l) - v(k-1, l))/(2 \cdot k \cdot h^2) \\ &\quad + (v(k, l+1) - 2 \cdot v(k, l) + v(k, l-1))/h^2 = 0. \end{aligned} \tag{3}$$

On the z-axis Eq. (1) reduces to the form

$$2 \cdot \frac{\partial^2 u(0, z)}{\partial r^2} + \frac{\partial^2 u(0, z)}{\partial z^2} = 0 \tag{4}$$

when the symmetry condition Equation (2) is used, instead of giving the boundary values $u(0, z)$. We therefore obtain for $k = 0$

$$\begin{aligned}&2 \cdot (2 \cdot v(1, l) - 2 \cdot v(0, l))/h^2 \\ &\quad + (v(0, l+1) - 2 \cdot v(0, l) + v(0, l-1))/h^2 = 0. \end{aligned} \tag{5}$$

The difference equations (3) and (5) approximate the Laplace equation (1) with a truncation error $\mathcal{O}(h^2)$.

We now assume that $u(r, z)$ can be expressed as a Fourier integral

$$u(r, z) = \frac{1}{(2\pi)^{1/2}} \cdot \int_{-\infty}^{+\infty} \hat{u}(r, \omega) \cdot \exp(i\omega z)\, d\omega$$

where $\hat{u}(r, \omega)$ is the Fourier transform of $u(r, z)$, or alternatively as a Fourier series

$$u(r, z) = \sum_{k=-\infty}^{+\infty} \hat{u}(r, k) \cdot \exp(ik\omega z)$$

where $\hat{u}(r, k)$ are the Fourier coefficients of $u(r, z)$. This is strictly valid only for problems where the region is an infinite strip along the z-axis with boundary data in $\mathscr{L}_2$, or problems which are periodic in z, with the period $L = 2\pi/\omega$. However, in many applications as, e.g., in the design of magnetic and electric lens systems in numerical electron optics, either of the two conditions is approximately satisfied.

In the work described in [1–3] and in [4, 5] the Laplace equation (1) is solved numerically in a rectangle centered around the z-axis. The boundary values of u at

the short sides $z = a$ and $z = b$ are constants or very nearly constants. If these two approximate constants are different, let us first subtract a linear function $A \cdot z + B$ from the boundary values. A and B are chosen such that the new constants for $z = a$ and $z = b$ are the same. Then the new problem has boundary data which are either in $\mathscr{L}_2$ or are periodic in z. The difference equation for the new problem can now be studied using Fourier techniques. But $A \cdot z + B$ is an exact solution to both the Laplace equation (1) and to any reasonable difference equation which approximates it. Therefore the results of the analysis of the modified problem are directly applicable to the original problem.

Fourier analysis of the Laplace equation (1) gives

$$\frac{\partial^2 \hat{u}(r, \omega)}{\partial r^2} + \frac{1}{r} \cdot \frac{\partial \hat{u}(r, \omega)}{\partial r} - \omega^2 \cdot \hat{u}(r, \omega) = 0$$

which has the general solution $A \cdot I_0(\omega r) + B \cdot K_0(\omega r)$, where I_0 and K_0 are the modified Bessel functions of order zero. But $I_0(\omega r) = 1 + \mathcal{O}((\omega r)^2)$ and $K_0(\omega r) = -\log(\omega r/2) + \mathcal{O}((\omega r)^2)$ according to relations 9.6.12 and 9.6.13 in [7]. From this we see that the we cannot in general specify both $\hat{u}(R, \omega)$ and $\hat{u}(0, \omega)$ to obtain values for A and B, i.e. we cannot in general specify both $u(R, z)$ and $u(0, z)$. We want to obtain a solution which is finite everywhere. Therefore $B = 0$ must hold. Thus it is possible to give values on the z-axis only if precisely the solution $u(0, z)$ resp. $\hat{u}(0, \omega)$ to the usual boundary value problem with symmetry at the z-axis is given.

Fourier analysis of the difference equations (3) and (5) now gives

$$\begin{aligned}(1 + 1/(2k)) \cdot \hat{v}(k + 1, \omega) - (4 - 2 \cdot \cos(\omega h)) \cdot \hat{v}(k, \omega) \\ + (1 - 1/(2k)) \cdot \hat{v}(k - 1, \omega) = 0 \qquad \text{for} \quad 1 \leqslant k \leqslant N - 1\end{aligned} \tag{6}$$

and when the symmetry condition is used

$$\hat{v}(1, \omega) - (3 - \cos(\omega h))/2 \cdot \hat{v}(0, \omega) = 0 \tag{7}$$

where $\hat{v}(k, \omega)$ is the Fourier transform of the difference solution $v(k \cdot h, l \cdot h) = v(r, z)$. We will in the following always use $R = 1$, i.e., $N \cdot h = 1$.

The difference equations (6) and (7) form a system of linear equations which is easily solved using a standard band-solver, see, e.g., [8]. Figure 1 shows the solution to Eq. (6) when $\hat{v}(0, \omega) = 1$ and $\hat{v}(N, \omega) = 0$, for $N = 20$. In Fig. 2 the corresponding curves are shown for $N = 80$. Note that all the curves are very steep, also the curve for $\omega = 0$. The mathematical problem corresponding to the difference equation (6) used in Figs. 1–3 does not have any solution, with the boundary data used there, as was shown above. Therefore the difference solution does not approach any limiting curve in these cases, when the stepsize h is decreased. Figure 3 shows the solution to Eq. (6) when $\hat{v}(0, \omega) = 0$ and $\hat{v}(N, \omega) = 1$, for $N = 20$. Note here the behavior of the solution for small r-values and low frequencies.

The difference solution obtained when the symmetry condition equation (7) is used is shown in Fig. 4. Here $\hat{v}(N, \omega) = 1$ and $N = 20$. The curves are all equal to

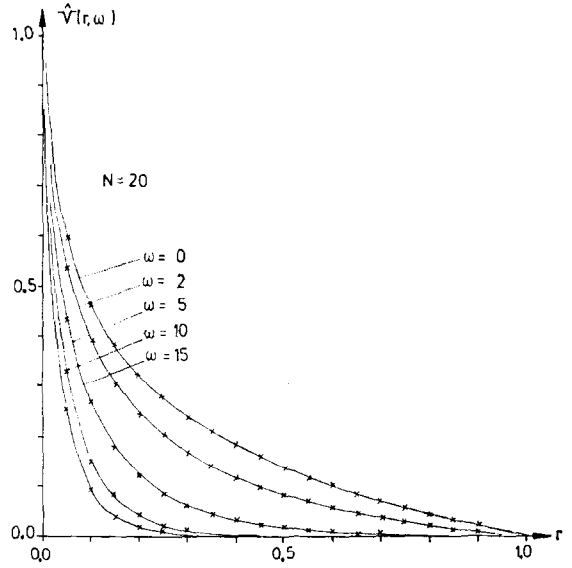

FIG. 1. The difference solution to the Fourier-transformed star 5-point formula for the Laplace equation in cylindrical coordinates. The boundary values are $\hat{v}(0, \omega) = 1$ and $\hat{v}(1, \omega) = 0$. The step size h is given by $N \cdot h = 1$, here $N = 20$. Note that all the curves are very steep, as is the curve for $\omega = 0$. The crosses in this and all the following figures denote the calculated values.

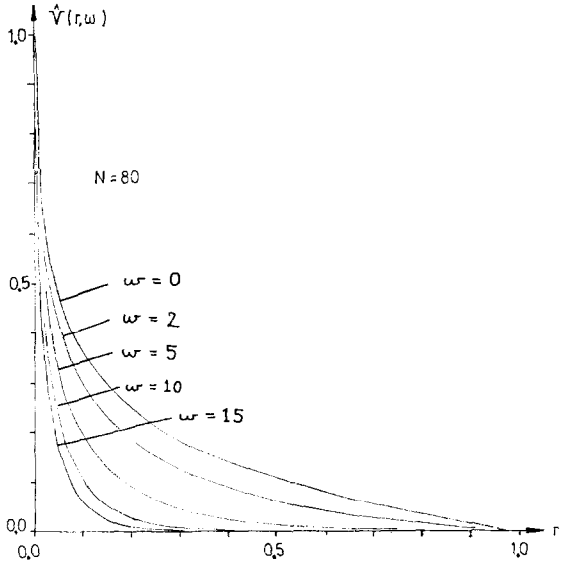

FIG. 2. The same as in Fig. 1, but $N = 80$. The mathematical problem corresponding to the difference equation used in Figs. 1–3 does not have any solution, with the boundary data used there. Therefore the difference solution does not approach any limiting curve as the step size h is decreased. The crosses denoting the calculated values have been omitted here.

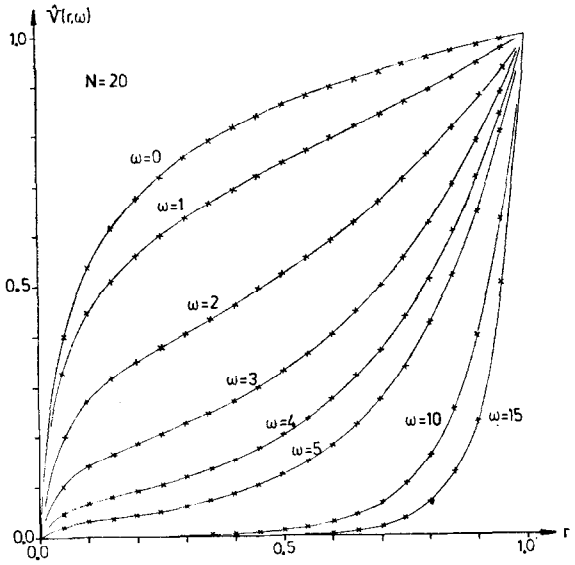

FIG. 3. The same as in Figs. 1 and 2, but the boundary values here are $\hat{v}(0, \omega) = 0$ and $\hat{v}(1, \omega) = 1$. Note the behavior of the solution for small r-values and low frequencies.

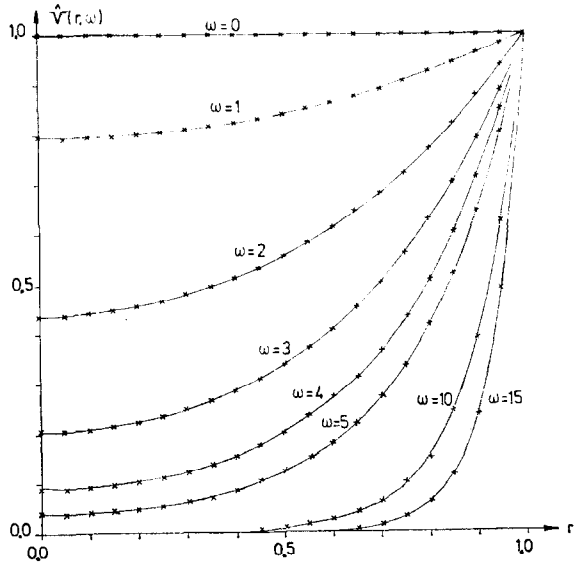

FIG. 4. The same as in Figs. 1–3, but the boundary data here are the symmetry condition $\partial\hat{u}(r, \omega)/\partial r = 0$ for $r = 0$, and $\hat{v}(1, \omega) = 1$. The curves are all equal to the mathematical solution $I_0(\omega r)/I_0(\omega)$ with good accuracy.

the mathematical solution $I_0(\omega r)/I_0(\omega)$ with good accuracy. A comparison with Fig. 3 shows that the two figures are very similar for $\omega \geqslant 4$ except for small r-values.

Let us now examine the work described in [1, 2, 3] more closely. The boundary values $v(r, z)$ were there all measured data on the z-component of the field in a magnetic lens spectrometer. The z-axis was used as a boundary with the boundary values $v(0, z)$ and the symmetry condition equation (2) was not used at all. If the measuring errors in the boundary data are negligibly small this problem has a mathematical solution and a smooth numerical solution. Let $v(r, z) = u(r, z) + \epsilon(r, z)$ where (r, z) denotes a point on the boundary, $\epsilon(r, z)$ is the measuring error in $v(r, z)$ and $u(r, z)$ is the correct (unknown) value. The boundary data $u(r, z)$ correspond to a solution u, which satisfies the Laplace equation (1).

Since the differential equation (1) is linear in u, we can separately analyze the effect of the errors $\epsilon(r, z)$, on the solution to the difference equation. We will here only consider the Fourier transform $\hat{\epsilon}(r, \omega)$, since we have no data on the size and distribution of $\epsilon(r, z)$. The measuring errors consist of systematic and random errors, which correspond mainly to low frequencies ($\omega \approx 0, 1, 2$) and high frequencies respectively. The difference solution $\hat{\epsilon}(r, \omega)$ is equal to $\hat{\epsilon}(0, \omega) \cdot \hat{v}(r, \omega)$ from Fig. 1 + $\hat{\epsilon}(1, \omega) \cdot \hat{v}(r, \omega)$ from Fig. 3. We now see that the total solution $\hat{\epsilon}(r, \omega)$ will vary rapidly close to the z-axis for all frequencies ω. The total influence $\epsilon(r, z)$ of the errors in the boundary data, is therefore not smooth close to the z-axis, but a "boundary layer" is formed.

The errors $\epsilon(0, z)$ are in [1, 2, 3] smaller than $\epsilon(1, z)$ since the measurements are easier to carry out on the z-axis. The formation of the boundary layer is therefore not very harmful for the total accuracy in this case. It is quite clear, however, that nothing at all is gained by using the boundary values $v(0, z)$ instead of the symmetry condition equation (2). The number of storage locations in the computer is also exactly the same. In addition, the measuring work is reduced in the symmetric case. Note that according to Fig. 1 the errors $\epsilon(0, z)$ have a very local influence on the total error. The high accuracy in the boundary data on the z-axis is therefore of little practical use.

In the work described in [1, 2, 3] the r-component of the magnetic field strength was also calculated. The differential equation

$$\frac{\partial^2 u}{\partial r^2} + \frac{1}{r} \cdot \frac{\partial u}{\partial r} + \frac{\partial^2 u}{\partial z^2} = \frac{u}{r^2}$$

was solved using a 5-point formula similar to Eqs. (3), (5). However, u vanishes identically on the z-axis because of the rotational symmetry ($u(r, z) = A(z) \cdot r + \mathcal{O}(r^3)$). This is therefore an ordinary elliptic boundary value problem and no "boundary layer" will occur at the z-axis.

Let us now consider the corresponding problem in a Cartesian (y, z)-coordinate system, where the z-axis is the symmetry axis. Fourier analysis of the Laplace equation

$$\frac{\partial^2 u(y, z)}{\partial y^2} + \frac{\partial^2 u(y, z)}{\partial z^2} = 0$$

now gives

$$\frac{\partial^2 \hat{u}(y, \omega)}{\partial y^2} - \omega^2 \cdot \hat{u}(y, \omega) = 0.$$

The general solution to this differential equation is $A \cdot \cosh(\omega y) + B \cdot \sinh(\omega y)$. For example, the solution corresponding to the boundary values $\hat{u}(0, \omega) = 1$, $\hat{u}(1, \omega) = 0$ is $\hat{u}(y, \omega) = \cosh(\omega y) - \sinh(\omega y)/\tanh(\omega)$ for $\omega \neq 0$ and $\hat{u}(y, 0) = 1 - y$. Therefore if boundary data are given on the symmetry axis in a Cartesian system the mathematical and numerical problems both have smooth solutions. However, the symmetry of the problem is then not used at all.

3. A Comparison between the Star 5-, Star 9-, and Compact 9-Point Formulas

If we calculate the difference solution to the Fourier transformed star 5-, star 9-, or compact 9-point formulas for the Laplace equation (1) using the symmetry condition equation (2) for $r = 0$ and $\hat{v}(1, \omega) = 1$, we obtain in each case the curves shown in Fig. 4. All the difference solutions therefore closely approximate the mathematical solution $\hat{u}(r, \omega) = I_0(\omega r)/I_0(\omega)$. Below we will calculate the error $\hat{e}(r, \omega) = |\hat{v}(r, \omega) - I_0(\omega r)/I_0(\omega)|$ for different frequencies ω, for the three Fourier-analyzed difference schemes. This enables us to compare the efficiency of the methods. This comparison holds strictly only under the assumptions on the boundary value problem, made in Section 2. However, in many practical problems these assumptions are approximately satisfied.

Figure 5 shows $^{10}\log \hat{e}(r, \omega)$ for the star 5-point formula, when $N = 20$. Note that the error increases almost exponentially with r, the more so the higher the frequency. All the curves in Figs. 5–7 end at $r = 1 - h$, since $e(1, \omega) = 0$ by definition. The value of the modified Bessel function $I_0(x)$ is calculated using Tables VII and XVII in [9]. This is the only paper giving useful approximations to $I_0(x)$ with an error $<10^{-15}$, for all values of x.

In [4], a star 9-point fromula is described which has been extensively used in calculations on electric two-tube lenses; see, e.g., [5]. The difference formulas used in [4] are:

$$\begin{aligned}
v_{0,j} &= (-v_{0,j-2} + 16 \cdot v_{0,j-1} + 16 \cdot v_{0,j+1} \\
&\quad - v_{0,j+2} + 64 \cdot v_{1,j} - 4 \cdot v_{2,j})/90, \\
v_{1,j} &= (-v_{1,j-2} + 16 \cdot v_{1,j-1} + 16 \cdot v_{1,j+1} \\
&\quad - v_{1,j+2} + 8 \cdot v_{0,j} + 24 \cdot v_{2,j} - 2 \cdot v_{3,j})/60, \\
v_{i,j} &= (-v_{i,j-2} + 16 \cdot v_{i,j-1} + 16 \cdot v_{i,j+1} - v_{i,j+2} \\
&\quad + (-1 + 1/i) \cdot v_{i-2,j} + (16 - 8/i) \cdot v_{i-1,j} \\
&\quad + (16 + 8/i) \cdot v_{i+1,j} + (-1 - 1/i) \cdot v_{i+2,j})/60,
\end{aligned}$$

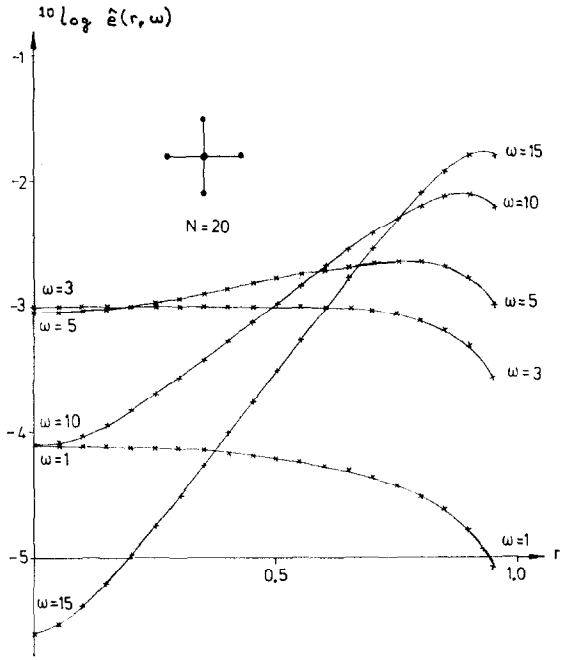

FIG. 5. The logarithm of the error $\hat{e}(r, \omega) = |\hat{v}(r, \omega) - I_0(\omega r)/I_0(\omega)|$ for the star 5-point formula for the Laplace equation in cylindrical coordinates. Note that the error increases almost exponentially with r, the more so the higher the frequency. The difference scheme is $\mathcal{O}(h^2)$.

for $2 \leqslant i \leqslant N - 2$, and

$$v_{N-1,j} = (-v_{N-1,j-2} + 16 \cdot v_{N-1,j-1} + 16 \cdot v_{N-1,j+1} - v_{N-1,j+2} + (12 - 6/(N-1)) \cdot v_{N-2,j} + (12 + 6/(N-1)) \cdot v_{N,j})/54,$$

where $v_{i,j} = v(r, z) = v(i \cdot h, j \cdot h)$ and $N \cdot h = 1$ as in Section 2. The formulas are all approximations to the Laplace equation (1) with a truncation error $\mathcal{O}(h^4)$, except for the last formulas at the boundary which is $\mathcal{O}(h^2)$. In the interior the difference molecule consists of 9 points arranged like a star. When we Fourier transform these difference equations we obtain, in the same way as in Section 2, a system of linear equations, which are easily solved. Figure 6 shows the logarithm of the error $\hat{e}(r, \omega)$ for different frequencies. Note that the exponential growth for high frequencies is enhanced compared to the star 5-point formula in Fig. 5. When comparing Figs. 5 and 6 it is easily seen that the star 9-point formula gives much higher accuracy than the star 5-point formula.

However, compact difference schemes are in general much better than broad difference schemes, also when the truncation errors are of the same power of h.

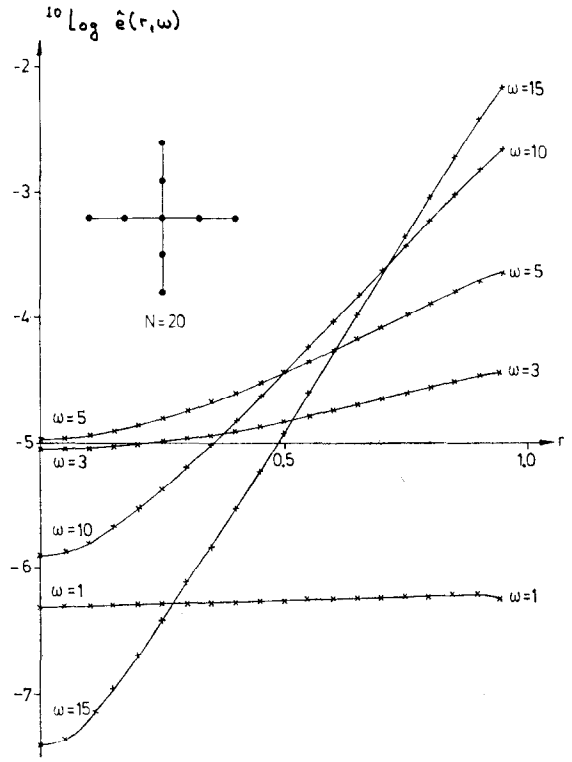

FIG. 6. The logarithm of the error $\hat{e}(r, \omega)$ for the star 9-point formula. The exponential growth of the error is much more pronounced here than in Fig. 5. The difference scheme is $\mathcal{O}(h^4)$, except at the boundary where it is $\mathcal{O}(h^2)$.

In addition, the approximation used at the boundary, which has a truncation error $\mathcal{O}(h^2)$, is known to give a $\mathcal{O}(h^4)$-contribution to the error in the interior points. This is of the same size as the error from the truncation term in the interior.

Let us therefore now consider the compact 9-point formula for the Laplace equation (1), which is given in [10]:

$$v_{0,j} = (5 \cdot v_{0,j-1} + 5 \cdot v_{0,j+1} + 7 \cdot v_{1,j-1} + 34 \cdot v_{1,j} + 7 \cdot v_{1,j+1})/58$$

and

$$\begin{aligned} v_{i,j} = [&(192 \cdot i^3 + 84 \cdot i) \cdot (v_{i,j-1} + v_{i,j+1}) \\ &+ (192 \cdot i^3 + 96 \cdot i^2 + 60 \cdot i + 46) \cdot v_{i+1,j} \\ &+ (192 \cdot i^3 - 96 \cdot i^2 + 60 \cdot i - 46) \cdot v_{i-1,j} \\ &+ (48 \cdot i^3 + 24 \cdot i^2 + 18 \cdot i + 13) \cdot (v_{i+1,j-1} + v_{i+1,j+1}) \\ &+ (48 \cdot i^3 - 24 \cdot i^2 + 18 \cdot i - 13) \cdot (v_{i-1,j-1} + v_{i-1,j+1})]/(960 \cdot i^3 + 360 \cdot i) \end{aligned}$$

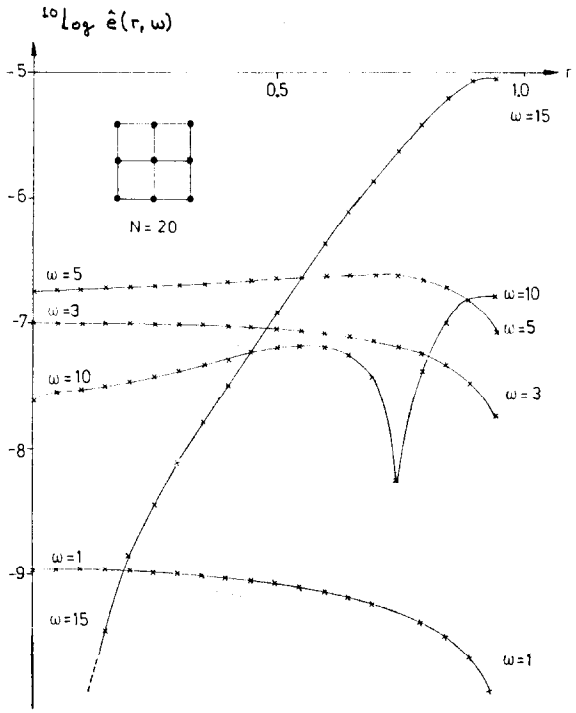

FIG. 7. The logarithm of the error $\hat{e}(r, \omega)$ for the compact 9-point formula. The error here is in general at least a factor of 100 smaller than in Fig. 6. The exponential growth of the error is slower than for the star 9-point formula. The sharp dip in the curve for $\omega = 100$ is caused by a change in sign of the error, and can therefore be completely neglected. The difference scheme is $\mathcal{O}(h^4)$, also at the boundary.

for $1 \leqslant i \leqslant N - 1$, where $v_{i,j} = v(r, z) = v(i \cdot h, j \cdot h)$ and $N \cdot h = 1$ as above. The truncation error is for both formulas $\mathcal{O}(h^4)$. Figure 7 shows the logarithm of the error $\hat{e}(r, \omega)$ for the Fourier transformed difference equations. The dip on the curve for $\omega = 10$ is caused by a change in the sign of the error and can therefore be ignored. A comparison with Fig. 6 shows that the error in the compact difference scheme is at least 100 times smaller for all frequencies than the error in the broad scheme. To our knowledge the compact formula has not been used at all in numerical electron optics, while the broad formula has been extensively used. Note also that a computer program for solving the Laplace equation (1) numerically is much simpler in structure when the compact scheme is used. Also, the round-off errors can accumulate in the broad scheme, since the sum of absolute values of the coefficients is $68/60 = 1.13$. This is never possible in the compact scheme, since all the coefficients there have the same sign. The actual gain in computer calculations with the compact scheme depends also on the time required to solve the large system of linear equations, using an iterative method or a band-solver.

It is easy to calculate the truncation terms for the broad and the compact schemes, if we first Fourier transform them. We then find that the compact scheme is better by a factor of 4 only, when $\omega = 0$, and about the same factor for higher frequencies. The great difference between Figs. 6 and 7 is caused, rather, by the error in the difference approximation at the boundary in the broad scheme. This error is propagated toward the interior and lowers the accuracy there. We confirmed this by recalculating Fig. 6 but now used the exact solution $I_0(\omega - \omega h)/I_0(\omega)$ in the point next to the boundary and did not use the boundary approximation at all. The result is shown in Fig. 8. A comparison between Figs. 7 and 8 shows that $\hat{e}(r, \omega)$ in Fig. 8 is slightly greater, which is in agreement with the difference in truncation error. In fact the forms of the curves in the two figures are almost the same for $\omega \leqslant 5$.

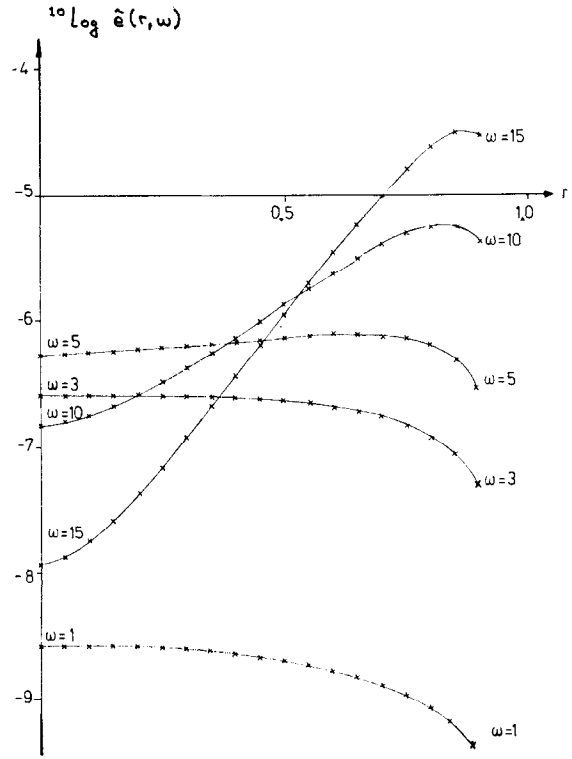

FIG. 8. The logarithm of the error $\hat{e}(r, \omega)$ for a modification of the star 9-point formula shown in fig. 6. The exact value $I_0(\omega - \omega h)/I_0(\omega)$ has been used in the point next to the boundary, instead of the boundary approximation, which is $\mathcal{O}(h^2)$. Therefore the error is identically equal to zero for $r = 1 - h$. Note that the forms of the curves are very similar to those in Fig. 7 for $\omega \leqslant 5$.

ACKNOWLEDGMENT

We would like to thank Professor Heinz-Otto Kreiss of the Department of Computer Sciences, Uppsala University, for his interest in this work.

REFERENCES

1. T. GROTH, B. OLSEN, AND G. PETTERSSON, *Nucl. Instrum. Methods* **56** (1967), 61.
2. T. GROTH, B. OLSEN, AND G. PETTERSSON, *Nucl. Instrum. Methods* **55** (1967), 93.
3. C. BESEV, T. GROTH, P. KLEINHEINZ, B. OLSEN, G. PETTERSSON, AND W. SCHNEIDER, *Nucl. Instrum. Methods* **62** (1968), 147.
4. S. NATALI, D. DI CHIO, AND C. E. KUYATT, *J. Res. Nat. Bur. Stand. USA Sect. A* **76** (1972), 27.
5. S. NATALI, D. DI CHIO, E. UVA, AND C. E. KUYATT, *Rev. Sci. Instrum.* **43** (1972), 80.
6. G. E. FORSYTHE AND W. R. WASOW, "Finite Difference Methods for Partial Differential Equations," Wiley, New York, 1960.
7. M. ABRAMOWITZ AND I. A. STEGUN, "Handbook of Mathematical Functions," Dover, New York, 1970.
8. Subroutine LEQT1B in the IMSL Library: International Mathematical and Statistical Libraries Inc., Sixth Floor, GNB Building, 7500 Bellaire Boulevard, Houston, Tex. 77036.
9. J. M. BLAIR, *Math. Comp.* **28**, No. 126 (1974), 581.
10. E. DURAND, *C. R. Acad. Sci. Paris* **244** (1957), 2355 (in French).

RECEIVED: April 1, 1977; REVISED: June 14, 1977

ANDERS SKÖLLERMO
Institute of Physics, Uppsala University
Box 530, S-751 21 Uppsala, Sweden

GUNILLA SKÖLLERMO
Department of Computer Sciences,
Uppsala University, Sturegatan 4 B,
S-752 23 Uppsala, Sweden